

This is a repository copy of *Incompatibility-Driven Self-Organization in Polycatenar Liquid Crystals Bearing Both Hydrocarbon and Fluorocarbon Chains*.

White Rose Research Online URL for this paper:

<https://eprints.whiterose.ac.uk/122005/>

Version: Published Version

---

**Article:**

Gainar, Adrian, Tzeng, Mei Chun, Heinrich, Benoît et al. (2 more authors) (2017) Incompatibility-Driven Self-Organization in Polycatenar Liquid Crystals Bearing Both Hydrocarbon and Fluorocarbon Chains. *Journal of Physical Chemistry B*. pp. 8817-8828. ISSN 1520-5207

<https://doi.org/10.1021/acs.jpcc.7b04490>

---

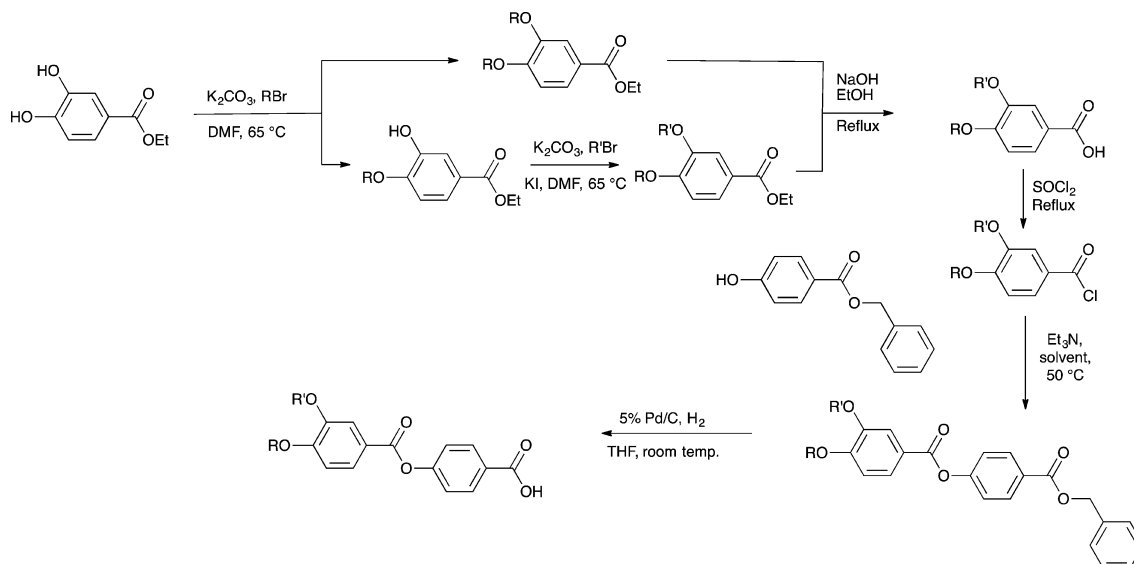
**Reuse**

Items deposited in White Rose Research Online are protected by copyright, with all rights reserved unless indicated otherwise. They may be downloaded and/or printed for private study, or other acts as permitted by national copyright laws. The publisher or other rights holders may allow further reproduction and re-use of the full text version. This is indicated by the licence information on the White Rose Research Online record for the item.

**Takedown**

If you consider content in White Rose Research Online to be in breach of UK law, please notify us by emailing [eprints@whiterose.ac.uk](mailto:eprints@whiterose.ac.uk) including the URL of the record and the reason for the withdrawal request.



Scheme 1. Summary of the Synthetic Route<sup>a</sup>

<sup>a</sup>Details are provided in the [Supporting Information](#).

tailed compounds as they form high-temperature, monolayer smectic A/C phases with undifferentiated alkyl and fluorinated layers, the differentiation appearing finally in the rectangular phases observed at lower temperature.<sup>32,33</sup> As a matter of fact, mesogens that are likely to form more two-dimensional mesophases (i.e., columnar phases) offer a potentially more intriguing prospect.<sup>34–37</sup>

Polycatenar mesogens, in particular, then present themselves as of interest in forming two-dimensional mesophases.<sup>38,39</sup> In particular, tetracatenar mesogens with 3,4-dialkoxyphenyl terminal groups are known to form a nematic (N) and lamellar (normally smectic C, SmC) phase at shorter chain lengths and a columnar phase at longer chain lengths, sometimes with a cubic phase at intermediate chain lengths.<sup>40</sup> This change from lamellar to columnar behavior has been explained<sup>41,42</sup> on the basis of the relative volume of the rigid core and of the terminal chains. Thus, as the chains occupy a greater volume either by getting longer or through increased thermal motion, there is an increasing mismatch between chain and core cross-sectional areas that leads to a breakup of a lamellar structure and the formation of what are conventionally described as columnar (Col) phases, normally with hexagonal or rectangular symmetry. We were then able to provide a thorough explanation of the organization in these columnar phases using detailed X-ray and dilatometric studies.<sup>43</sup> Given the depth of understanding of these polycatenar systems, they appeared the perfect choice to explore how formally amphiphilic materials might organize. The motif chosen is found in [Scheme 2](#) and consists of a core of five phenyl rings separated by ester functions. We have reported previously on all-hydrocarbon tetracatenar derivatives of these compounds,<sup>44</sup> and in this study, we have used synthetic approaches capable of generating unsymmetric derivatives to allow some systematic variations.

## ■ SYNTHESIS

The unsymmetric nature of many of the target compounds led to a modular approach to the synthetic chemistry, which is described in detail in the [Supporting Information](#) and is summarized in [Scheme 1](#). The semiperfluorinated alkyl chain

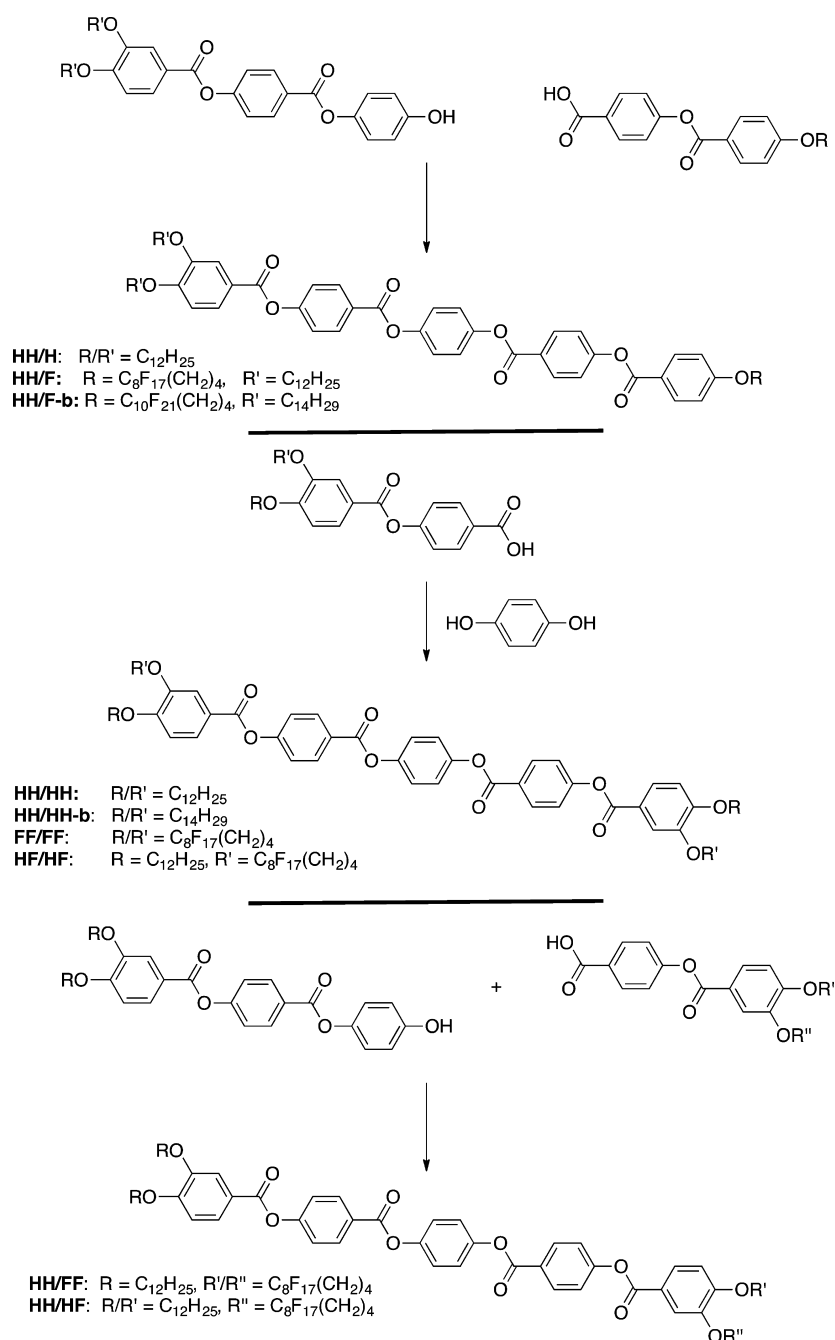
was introduced using a tetramethylene spacer following an approach described elsewhere.<sup>45–47</sup> Some of the target compounds contained an unsymmetrically difunctionalized 3,4-dialkoxybenzoate unit, and it is of interest to note its preparation ([Scheme 1](#)). It is also important to realize that the presence of long-chain perfluoroalkyl fragments reduces the solubility of the various compounds significantly, even when using solvents such as trifluoromethylbenzene,<sup>48</sup> and that this influenced aspects of the synthetic strategy. The final synthetic step to each product under consideration is shown in [Scheme 2](#), which also shows a labeling scheme.

## ■ MESOMORPHISM OF THE TARGET COMPOUNDS: OPTICAL AND STRUCTURAL STUDIES

First, it should be noted that several of the intermediate compounds have LC properties that have not been reported previously, and these are collected in the [Supporting Information](#).

The thermal behavior for the polycatenar compounds is collected in [Table 1](#) and summarized in a chart ([Figure 1](#)), with representative textures shown in [Figure 2](#). Experimental details of how these data were obtained are found in the [Supporting Information](#). Typical for such substitution patterns, the mesomorphism of the tricaténar compounds is dominated by the occurrence of the SmC phase, whereas for the tetracatenar homologues, both smectic and columnar mesophases are displayed.

Tricaténar compounds **HH/H** and **HH/F**<sup>†</sup> († implies either semiperfluorocarbon chain length) melt to liquid-crystalline phases, giving rise to fluid textures with characteristic broken fan and Schlieren areas, recognized readily as SmC phases ([Figure 2](#)). Consistent with the anisotropy of the molecular core, the clearing point was high at ~240 °C, although it was of interest to note that the melting point was as low as 132 °C. The compounds with only hydrocarbon terminal chains, that is, tricaténar compound **HH/H**, also showed a higher-temperature nematic phase. When the isolated hydrocarbon chain in the tricaténar compounds is replaced by a semiperfluorocarbon chain (**HH/F**), a slight enhancement of the mesomorphic

Scheme 2. Synthetic Routes to the Target Compounds, Final Step<sup>a</sup>

<sup>a</sup>The nomenclature represents the type of chain (H = hydrocarbon, F = semiperfluorocarbon). The total number of carbon atoms in the chain is always 12, either  $C_{12}H_{25}$ -(H) or  $C_8F_{17}(CH_2)_4$ -(F), except for two cases (indicated with -b at the end) where carbon chain lengths are 14 ( $C_{14}H_{29}$ - or  $C_{10}F_{21}(CH_2)_4$ -).

range is observed while the melting point remains almost the same. However, the nematic phase observed in **HH/H** has totally disappeared at the expense of the SmC phase, which takes over the entire mesomorphic domain.

The previously reported<sup>49</sup> tetracatenar compounds **HH/HH** also melt to SmC phases (Figure 1), with **HH/HH** also showing a higher-temperature nematic phase while **HH/HH-b** also exhibits a lower-temperature Col<sub>r</sub> phase.<sup>49</sup> If one of the *meta*-alkyl chains of the tetracatenar compound **HH/HH** is replaced by a semiperfluorinated fragment (**HH/HF**), the crystalline phase is destabilized, leading to an increase in the

mesophase temperature range from less than 8 °C to about 22 °C (**HH/HH** vs **HH/HF**). This modification also affects the organization of the molecules in the mesophase as, based on the optical texture, the phase is Col<sub>h</sub> (Figure 2, vide infra).

The two isomeric tetracatenar mesogens with two alkyl and two semiperfluorinated chains behaved rather differently. Tetracatenar **HH/FF**, with two dodecyloxy chains at one end and two semiperfluoroalkyl chains at the other, melts at a slightly higher temperature (138.6 °C) than the isomeric compound **HF/HF** (128.3 °C) into a SmC phase with a rather extended range. Upon further heating, a second transition leads

**Table 1.** Thermal behavior of the compounds discussed in this study

compounds	transition <sup>b</sup>	T/°C	$\Delta H/\text{kJ mol}^{-1}$
HH/H	Cr–SmC	131.8	34.5
	SmC–N	220.0	8.0
	N–Iso	241.5	1.8
HH/F	Cr–SmC	131.5	42.7
	SmC–Iso	248.1	9.0
HH/F-b	Cr–SmC	137.1	51.68
	SmC–Iso	251.2	12.73
HH/HH <sup>a</sup>	Cr–SmC	162.5	73.7
	SmC–N	170.2	4.7
	N–Iso	171.9	0.7
HH/HH-b <sup>a</sup>	Cr–Col <sub>r</sub>	154.0	72.2
	Col <sub>r</sub> –SmC	162.7	0.6
	SmC–Iso	164.3	8.2
FF/FF	Cr–Cr <sub>1</sub>	117.9	–12.2
	Cr <sub>1</sub> –Col <sub>h</sub>	137.4	23.1
	Col <sub>h</sub> –Iso	259.5	3.3
HH/FF	Cr–Cr <sub>1</sub>	112.5	3.2
	Cr <sub>1</sub> –SmC	138.6	45.9
	SmC–Col <sub>r</sub>	171.1	2.3
	Col <sub>r</sub> –Iso	208.2	3.6
HF/HF	Cr–Cr <sub>1</sub>	94.5	1.93
	Cr <sub>1</sub> –Cr <sub>2</sub>	120.4	11.3
	Cr <sub>2</sub> –Col <sub>h</sub>	128.3	9.1
	Col <sub>h</sub> –Iso	169.9	3.7
HH/HF	Cr–Cr <sub>1</sub>	105.0	1.09
	Cr <sub>1</sub> –Col <sub>h</sub>	152.6	53.5
	Col <sub>h</sub> –Iso	174.1	5.2

<sup>a</sup>Data from ref 49. <sup>b</sup>Cr, Cr<sub>1</sub>, Cr<sub>2</sub>: crystalline phases; SmC: smectic C phase; N: nematic phase; Col<sub>r</sub>: rectangular columnar phase; Col<sub>h</sub>: hexagonal columnar phase; Iso: isotropic liquid.

to another mesophase that persists for over 30 °C before clearing is observed at 208.2 °C; this second mesophase was assigned as a columnar phase (vide infra) on the basis of optical microscopy (Figure 2). Isomeric compound HF/HF, which bears a semiperfluorinated chain in the two terminal meta positions and hydrocarbon chains in the para positions, melts at 128.3 °C to give a mesophase that persists up to 169.9 °C. The optical texture (Figure S3) shows clearly that the phase is columnar, and the presence of large homeotropic zones even suggests that phase symmetry is hexagonal, Col<sub>h</sub>. It is interesting to note that the lower melting and clearing points of HF/HF compared to HH/FF implies that the mixing of terminal (*para*-)hydrocarbon and lateral (*meta*-)semiperfluorocarbon chains is disruptive both to the packing in the crystal phase and to the organization in the mesophase. That a *meta*-semiperfluoroalkyl chain is disruptive to crystal-phase organization is also shown when compound HH/HF is considered, which is a tetracatenar mesogen bearing three hydrocarbon chains and one semiperfluoroalkyl chain in a meta position. Thus, while the clearing points of HH/HH and HH/HF are remarkably similar (171.9 vs 174.1 °C, respectively), the melting point of HH/HF is reduced compared to that of HH/HH (152.6 vs 170.2 °C, respectively). Furthermore, the mesomorphism changes from SmC and N in HH/HH to Col<sub>h</sub> in HH/HF.

Finally, the tetracatenar compound bearing four semiperfluorinated chains (FF/FF) was found to exhibit a single columnar hexagonal phase over a substantial temperature range.

Thus, compound FF/FF melts at 137.4 °C, a temperature appreciably lower than that of the analogous all-hydrocarbon analogue HH/HH, and clears at 259.5 °C, displaying the broadest temperature range of this series of compounds, of ~122 °C.

The 1,4-phenylene-bis(4-(benzoyloxy)benzoate) structure is therefore a suitable molecular building block to design LC materials,<sup>49</sup> as revealed by the rich and diverse mesomorphism exhibited by both series of polycatenar mesogens. Whereas the tricatener mesogens show a wide mesomorphic range on account of relatively low melting points and high mesophase stability, grafting of an additional aliphatic chain to give tetracatenar materials in general lead to destabilization of the clearing point, while melting points are similar or slightly higher except for FF/FF with four semiperfluoroalkyl chains, where the mesophase range recovers close to those of tricatener mesogens HH/H and HH/F. As expected, moving from tricatener systems to those that are tetracatenar leads to an evolution of the mesomorphism away from simply SmC and N to include ribbon and columnar phases, too (Figure 1). The nature of this evolution forms the basis for the following discussion.

## ■ SMALL-ANGLE X-RAY SCATTERING (SAXS): SUPRAMOLECULAR ORGANIZATION

The polycatenar compounds were studied by SAXS, and the data and mesophase parameters are collected in Table 2. For the all-hydrocarbon compound HH/H, the diffraction pattern recorded at 140 °C showed only a single, low-angle reflection, which, supported by microscopy, can be attributed to the lamellar periodicity of a SmC phase of  $\sim 36.85 \pm 0.15$  Å (001), and a broad, wide-angle signal that corresponds to a spacing of 4.6 Å,  $h_{\text{max}}$  reflecting the superposition of the molten aliphatic chains,  $\langle h_{\text{H}} \rangle$ , and mesogenic core,  $\langle h_{\text{c}} \rangle$  (Figure 3). For the tricatener compounds with the semiperfluorinated chain (HH/F and HH/F-b), several orders of lamellar reflections (00 $l$ ), up to  $l = 3$  (HH/F) and  $l = 6$  (HH/F-b), are observed, suggesting well-organized layers with sharp interfaces in the mesophases. The diffuse reflection at wide angle is also present but broader and slightly shifted to smaller angle ( $\sim 5.0$  Å) as a result of the superposition of the reflections from the molten hydrocarbon/core  $\langle h_{\text{H}} \rangle$  and fluorocarbon  $\langle h_{\text{F}} \rangle$  chains, whose maxima are expected at 4.76, 4.73, and 5.77 Å, respectively (Figure 3, Table 2). Indeed, the theoretical position of the scattering maximum is notably different for semiperfluorocarbon chains and hydrocarbon chains (the latter coinciding with mesogens), but contributions are not resolved and only a broad maximum is observed whose position depends on the proportion of semiperfluorocarbon chains (Figures 3 and 4).

The SAXS data for HH/FF at various temperatures confirm the presence of two mesophases. The lamellar nature of the lower-temperature phase was deduced from the presence of three small-angle reflections in a 1:2:3 ratio, again suggesting well-correlated layers, along with the broad halo,  $h_{\text{max}}$  at wide angles (Figure 2). The obvious feature when comparing HH/H with the other smectogens HH/F and HH/FF is the almost exact doubling of the lamellar periodicity in HH/F (76.4 Å), HH/F-b (82.3 Å), and HH/FF (76 Å), suggesting bilayer organization in these last three. The distinctly amphiphilic nature of HH/F and HH/FF likely imposes this organization owing to the mutual immiscibility of the terminal hydrocarbon and fluorocarbon chains.



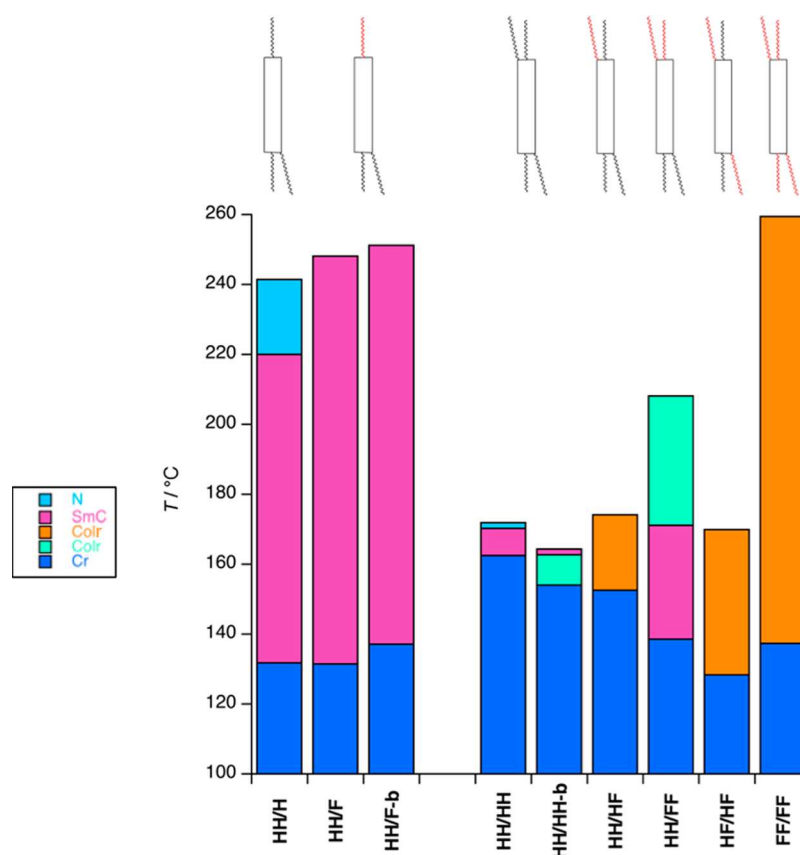


**Figure 1.** Bar chart showing mesophase temperatures for the compounds under study, along with a schematic molecular drawing in which hydrocarbon chains are indicated in black and fluorocarbon chains in red.

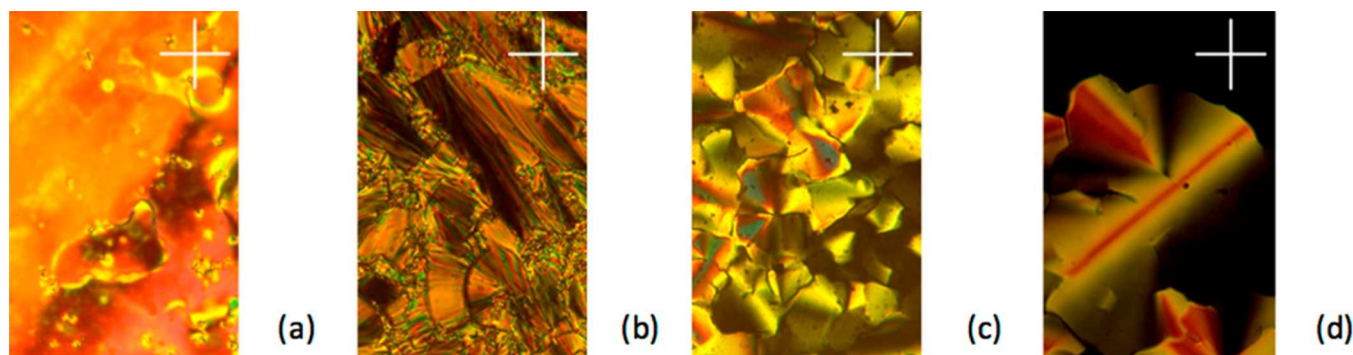


**Figure 2.** Representative optical micrographs (all textures obtained upon cooling – the white cross indicates the direction of the polarizers): (a) nematic phase of HH/HH at 220 °C, (b) SmC phase of HH/F at 160 °C, (c) Col<sub>h</sub> phase of FF/FF at 160 °C, (d) Col<sub>h</sub> phase of HH/HF at 150 °C.

SAXS investigations of the other tetracatenar mesogens also confirm their LC nature (Figure 3). They are all characterized by strong diffuse wide-angle scattering with a maximum of diffusion at  $\sim 5.1$ – $5.5$  Å ( $h_{\max}$ ), which corresponds, as mentioned already, to the superposition of the diffuse signals  $\langle h_H \rangle$ ,  $\langle h_F \rangle$ , and  $\langle h_c \rangle$ .

The SAXS pattern of FF/FF at 180 °C confirms the hexagonal nature of the mesophase, revealing small-angle reflections with relative spacings  $1:\sqrt{3}:\sqrt{7}$  and the lattice parameter  $a = 53.1$  Å. In this case, the diffraction pattern shows rather low-intensity reflections (Figure 3) on account of there being little electronic contrast between the unsaturated rings in the core of the molecule and the perfluorocarbon fragments at the extremities, which are only separated by a very small volume fraction of aliphatic spacer (of lower electronic

density). The lattice parameter is almost constant across the temperature range.

For the higher-temperature phase of HH/FF (vide supra), there are enough reflections to enable identification of the phase symmetry, and the assignment of the two observed reflections as (20)/(11) and (12) is in agreement with a noncentered, rectangular lattice ( $p2gg$ ). The lack of centrosymmetry is ascertained by the presence of the (12) reflection (this excludes centering on the basis of the extinction rule:  $h + k = 2n + 1$ ). It is likely that this phase arises from modulation of the underlying lamellar phase to give a superlattice with  $a = 160.3$  Å and  $b = 92.5$  Å ( $a/b = \sqrt{3}$ ). The isomeric compound, HF/HF, showed only a single, small-angle reflection, which, supported by microscopy, confirms the presence of the Col<sub>h</sub> mesophase. However, the fundamental reflection shows

Table 2. X-ray and Structural Data for the Mesophases of the Polycatenar Mesogens<sup>a</sup>

$d_{\text{meas}}/\text{\AA}$	$hkl$	intensity	$d_{\text{calc}}/\text{\AA}$	parameters
<b>HH/H</b>				
36.85	001	VS (sh)	36.85	$T = 140\text{ }^{\circ}\text{C}$ , SmC
4.6	—	VS (br)	$h_{\text{max}}$	$d = 36.85\text{ \AA}$ ( $N_L = 1$ ) $V_{\text{mol}} = 1870\text{ \AA}^3$ ( $\rho = 0.99$ ) $A_{\text{mol}} = 50.7\text{ \AA}^2$ $a_{\text{C}}, \sigma_{\text{C}} = 50.7, 23.5\text{ \AA}^2$ ; $\psi_{\text{C}} = 62^{\circ}$ $a_{\text{H}}, \sigma_{\text{H}} = 33.8, 23.1\text{ \AA}^2$ ; $q_{\text{H}} = 1.46$ $\langle h_{\text{C}} \rangle, \langle h_{\text{H}} \rangle = 4.73, 4.70\text{ \AA}$
<b>HH/F</b>				
76.0	001	VS (sh)	76.43	$T = 160\text{ }^{\circ}\text{C}$ , SmC
38.37	002	S (sh)	38.21	$d = 76.4\text{ \AA}$ ( $N_L = 2$ )
25.5	003	M (sh)	25.47	$V_{\text{mol}} = 2060\text{ \AA}^3$ ( $\rho = 1.14$ )
5.0	—	VS (br)	$h_{\text{max}}$	$A_{\text{mol}} = 27.0\text{ \AA}^2$ $a_{\text{C}}, \sigma_{\text{C}} = 54.0, 23.8\text{ \AA}^2$ ; $\psi_{\text{C}} = 64^{\circ}$ $a_{\text{H}}, \sigma_{\text{H}} = 27.0, 23.5\text{ \AA}^2$ ; $q_{\text{H}} = 1.15$ $a_{\text{F}}, \sigma_{\text{F}} = 54.0, 34.9\text{ \AA}^2$ ; $q_{\text{F}} = 1.55$ $\langle h_{\text{C}} \rangle, \langle h_{\text{H}} \rangle, \langle h_{\text{F}} \rangle = 4.76, 4.73, 5.77\text{ \AA}$
<b>HH/F-b</b>				
81.9	001	VS (sh)	82.30	$T = 160\text{ }^{\circ}\text{C}$ , SmC
41.38	002	S (sh)	41.15	$d = 82.3\text{ \AA}$ ( $N_L = 2$ )
27.46	003	M (sh)	27.43	$V_{\text{mol}} = 2270\text{ \AA}^3$ ( $\rho = 1.15$ )
20.58	004	VW (sh)	20.57	$A_{\text{mol}} = 27.6\text{ \AA}^2$
16.45	005	M (sh)	16.46	$a_{\text{C}}, \sigma_{\text{C}} = 55.2, 23.8\text{ \AA}^2$ ; $\psi_{\text{C}} = 65^{\circ}$
13.7	006	W (sh)	13.72	$a_{\text{H}}, \sigma_{\text{H}} = 27.6, 23.5\text{ \AA}^2$ ; $q_{\text{H}} = 1.18$
5.0	—	VS (br)	$h_{\text{max}}$	$a_{\text{F}}, \sigma_{\text{F}} = 55.2, 34.9\text{ \AA}^2$ ; $q_{\text{F}} = 1.58$ $\langle h_{\text{C}} \rangle, \langle h_{\text{H}} \rangle, \langle h_{\text{F}} \rangle = 4.76, 4.73, 5.77\text{ \AA}$
<b>FF/FF</b>				
46.26	10	M (sh)	45.96	$T = 160\text{ }^{\circ}\text{C}$ , Col <sub>h</sub>
26.73	11	M (sh)	26.53	$a = 53.1\text{ \AA}$ ; $A = 2440\text{ \AA}^2$ ( $Z = 1$ )
17.33	21	M (sh)	17.37	$V_{\text{mol}} = 2940\text{ \AA}^3$ ( $\rho = 1.42$ )
5.5	—	VS (br)	$h_{\text{max}}$	$S = 2440\text{ \AA}^2$ ; $h_{\text{mol}} = 1.21\text{ \AA}$ ; $N_{\text{C}} = 4.6$ $a_{\text{Cyl1,H}}, \sigma_{\text{H}} = 26.4, 23.5\text{ \AA}^2$ ; $q_{\text{H}} = 1.13$ $a_{\text{Cyl2,F}}, \sigma_{\text{F}} = 33.9, 34.9\text{ \AA}^2$ ; $q_{\text{F}} = 0.97$ $\langle h_{\text{C}} \rangle, \langle h_{\text{H}} \rangle, \langle h_{\text{F}} \rangle = 4.76, 4.73, 5.77\text{ \AA}$
<b>HH/FF</b>				
76.0	001	VS (sh)	75.90	$T = 160\text{ }^{\circ}\text{C}$ , SmC
37.95	002	S (sh)	37.95	$d = 75.9\text{ \AA}$ ( $N_L = 2$ )
25.3	003	M (sh)	25.30	$V_{\text{mol}} = 2600\text{ \AA}^3$ ( $\rho = 1.22$ )
5.2	—	VS (br)	$h_{\text{max}}$	$A_{\text{mol}} = 34.3\text{ \AA}^2$ $a_{\text{C}}, \sigma_{\text{C}} = 68.5, 23.8\text{ \AA}^2$ ; $\psi_{\text{C}} = 70^{\circ}$ $a_{\text{H}}, \sigma_{\text{H}} = 34.3, 23.5\text{ \AA}^2$ ; $q_{\text{H}} = 1.46$ $a_{\text{F}}, \sigma_{\text{F}} = 34.3, 34.9\text{ \AA}^2$ ; $q_{\text{F}} = 0.98$ $\langle h_{\text{C}} \rangle, \langle h_{\text{H}} \rangle, \langle h_{\text{F}} \rangle = 4.76, 4.73, 5.77\text{ \AA}$
80.3	11/20	VS (sh)	80.15	$T = 200\text{ }^{\circ}\text{C}$ , Col <sub>t</sub>
44.4	12	S (br)	44.46	$a, b = 160.3, 92.5\text{ \AA}$ ; $A = 14840\text{ \AA}^2$ ( $Z = 6$ )
5.4	—	—	$h_{\text{max}}$	$V_{\text{mol}} = 2680\text{ \AA}^3$ ( $\rho = 1.18$ ) $S = 2473\text{ \AA}^2$ ; $h_{\text{mol}} = 1.08\text{ \AA}$ ; $N_{\text{C}} = 5.0$ $a_{\text{Cyl1,H}}, \sigma_{\text{H}} = 25.2, 24.1\text{ \AA}^2$ ; $q_{\text{H}} = 1.04$ $a_{\text{lay,F}}, \sigma_{\text{F}} = 33.4, 35.9\text{ \AA}^2$ ; $q_{\text{F}} = 0.93$ $\langle h_{\text{C}} \rangle, \langle h_{\text{H}} \rangle, \langle h_{\text{F}} \rangle = 4.82, 4.79, 5.85\text{ \AA}$
<b>HF/HF</b>				
44.25	10	VS (sh)	44.25	$T = 140\text{ }^{\circ}\text{C}$ , Col <sub>h</sub>
19	—	S ( $\xi = 25\text{ \AA}$ )	$D$	$a = 51.1\text{ \AA}$ ; $A = 2261\text{ \AA}^2$ ( $Z = 1$ )
5.1	—	VS (br)	$h_{\text{max}}$	$V_{\text{mol}} = 2570\text{ \AA}^3$ ( $\rho = 1.23$ ) $S = 2261\text{ \AA}^2$ ; $h_{\text{mol}} = 1.14\text{ \AA}$ ; $N_{\text{C}} = 4.5$ $a_{\text{Cyl1,H}}, \sigma_{\text{H}} = 25.6, 23.1\text{ \AA}^2$ ; $q_{\text{H}} = 1.11$ $a_{\text{Cyl2,H/F}}, \sigma_{\text{H/F}} = 32.8, 28.8\text{ \AA}^2$ ; $q_{\text{H/F}} = 1.14$ $\langle h_{\text{C}} \rangle, \langle h_{\text{H}} \rangle, \langle h_{\text{F}} \rangle = 4.73, 4.70, 5.73\text{ \AA}$
<b>HH/HF</b>				
42.33	10	S (sh)	42.33	$T = 150\text{ }^{\circ}\text{C}$ , Col <sub>h</sub>
19	—	S ( $\xi = 25\text{ \AA}$ )	$D$	$a = 48.9\text{ \AA}$ ; $A = 2069\text{ \AA}^2$ ( $Z = 1$ )

Table 2. continued

$d_{\text{meas}}/\text{\AA}$	$hkl$	intensity	$d_{\text{calc}}/\text{\AA}$	parameters
			<b>HH/HF</b>	
5.2	—	VS (br)	$h_{\text{max}}$	$V_{\text{mol}} = 2420 \text{ \AA}^3$ ( $\rho = 1.10$ ) $S = 2069 \text{ \AA}^2$ ; $h_{\text{mol}} = 1.17 \text{ \AA}$ ; $N_c = 4.4$ $a_{\text{cyl1,H}} \sigma_{\text{H}} = 26.0, 23.3 \text{ \AA}^2$ ; $q_{\text{H}} = 1.12$ $a_{\text{cyl2,H/F}} \sigma_{\text{H/F}} = 33.3, 25.8 \text{ \AA}^2$ ; $q_{\text{H/F}} = 1.29$ $\langle h_c \rangle, \langle h_H \rangle, \langle h_F \rangle = 4.74, 4.71, 5.75 \text{ \AA}$

$d_{\text{meas}}$  and  $d_{\text{calc}}$  are the measured and calculated diffraction spacings [ $d_{\text{calc}}$  is deduced from the following mathematical expressions  $d_{00l} = 1/N_l(\sum d_{00l} \times l)$ , where  $N_l$  is the number of 00l reflections observed for the lamellar phases;  $a = 2(\sum d_{hk} \times (h^2 + k^2 + hk)^{1/2}/N_{hk})\sqrt{3}$ , where  $N_{hk}$  is the number of  $hk$  reflections observed for the Col<sub>h</sub> phase,  $1/d_{hk} = \sqrt{(h^2/a^2 + k^2/b^2)}$  for the Col<sub>h</sub>].  $hkl$  are the Miller indices of the reflections corresponding to the lamellar (00l) and columnar ( $hk$ ) phases, respectively. Intensity of the sharp reflections: VS, very strong; S, strong; M, medium; VW, very weak; sh and br stand for sharp and broad reflections;  $h_{\text{max}}$  is the position of the wide-angle scattering maximum, which is the superposition of the contributions from molten hydrocarbon ( $h_H$ ), core ( $h_c$ ), and fluorocarbon ( $h_F$ ) layers;  $D$  is a short-range correlated periodicity ( $\xi$ : correlation length from the Scherrer equation).  $V_{\text{mol}}$ ,  $\sigma_c$ ,  $\sigma_H$ ,  $\sigma_F$ : calculated molecular volume ( $\rho$  corresponding density in  $\text{g cm}^{-3}$ ) and natural cross sections, obtained from reference dilatometric measurements;<sup>26,41</sup>  $\langle h_c \rangle$ ,  $\langle h_H \rangle$ ,  $\langle h_F \rangle$ : average lateral distance between molten segments, calculated from equation  $\langle h_i \rangle = 0.9763\sigma_i^{0.5}$ , where  $i = \text{C, H, and F}$ ;<sup>50</sup> SmC phase:  $d$ ,  $N_L$ : periodicity of the SmC phase and number of molecular layers per lamella;  $A_{\text{mol}} = V_{\text{mol}}/d$ : molecular area;  $a_c = A_{\text{mol}}N_L/n_c$ ,  $a_H = A_{\text{mol}}N_L/n_H$ ,  $a_F = A_{\text{mol}}N_L/n_F$ : layer areas covered by single mesogen, alkyl chain, and fluorinated chain, with  $n_F$ ,  $n_c$ , and  $n_H$  being the number of C, F, or H segments per sublayer, respectively (for HH/H, HH/F, HH/F-b, HH/FF:  $n_c = 1, 1, 1, 1$ ;  $n_H = 3/2, 2, 2, 2$ ;  $n_F = 0, 1, 1, 2$ );  $\psi_c = \arccos(\sigma_c/a_c)$ : average polar tilt angle of mesogenic cores inside the lamellae;  $q_H = a_H/\sigma_H$ ,  $q_F = a_F/\sigma_F$ : chain packing ratios ( $q_i = 1$  for flat layers and fully stretched chains). Col<sub>r</sub> and Col<sub>h</sub> phases:  $a$ ,  $b$ : lattice parameters ( $a$ ,  $b$  in the Col<sub>r</sub> phase,  $a = b$  in the Col<sub>h</sub> phases);  $A$ ,  $Z$ : lattice area and number of columns of mesogenic cores per lattice;  $S = A/Z$ : area per column;  $h_{\text{mol}} = V_{\text{mol}}/S$ : molecular slice thickness (i.e., the height of the column segment equivalent to that of a single molecule);  $N_c = h_{\text{max}}/h_{\text{mol}}$ : number of aggregated molecules per columnar section, for intermolecular distance  $h_{\text{max}}$ .  $a_{\text{cyl1,H}} = \pi(4/\pi x_c S)^{0.5} h_{\text{mol}}/n_{\text{H/F}}$ : area per alkyl spacer at the interface between columnar cores and an internal aliphatic shell assuming cylindrical column shape,  $x_c$  being the volume fraction of the mesogenic cores (HH/FF, FF/FF, HH/HF, HF/HF:  $x_c = 0.2774, 0.2507, 0.3035, 0.2851$ );  $q_H = a_{\text{cyl1,H}}/\sigma_H$ : chain packing ratio of the alkyl spacers near the interface.<sup>51,52</sup>  $a_{\text{lay,F}} = bh_{\text{mol}}/(Z/N_{\text{lay,F}})$ : layer area covered by a single fluorinated chain in the Col<sub>r</sub> phase of HH/FF,  $N_{\text{lay,F}}$  being the number of fluorinated layers per lattice ( $N_{\text{lay,F}} = 2$ );  $q_F = a_{\text{lay,F}}/\sigma_F$ : chain packing ratio of the fluorinated chains.  $a_{\text{cyl2,H/F}} = \pi(4/\pi x_{\text{CH}} S)^{0.5} h_{\text{mol}}/n_{\text{H/F}}$ : area per terminal chain at the boundary between the internal aliphatic shell and the external F shell (FF/FF) or mixed F/H (HF/HF, HH/HF) shell in the Col<sub>h</sub> phases, the boundary shape being assumed cylindrical and  $x_{\text{CH}}$  representing the total volume fraction of mesogenic cores, alkyl spacers of F tails and segments of H tails of same length as spacers (FF/FF, HH/HF, HF/HF:  $x_{\text{CH}} = 0.4128, 0.4990, 0.4681$ ).  $\sigma_{\text{H/F}} = (n_H\sigma_H + n_F\sigma_F)/(n_H + n_F)$ : average cross section of the terminal chains,  $n_H$  and  $n_F$  being the number of H and F tails in a molecule;  $q_{\text{H/F}} = a_{\text{cyl2,H/F}}/\sigma_{\text{H/F}}$ : chain packing ratio of terminal chains near the boundary with the internal shell.

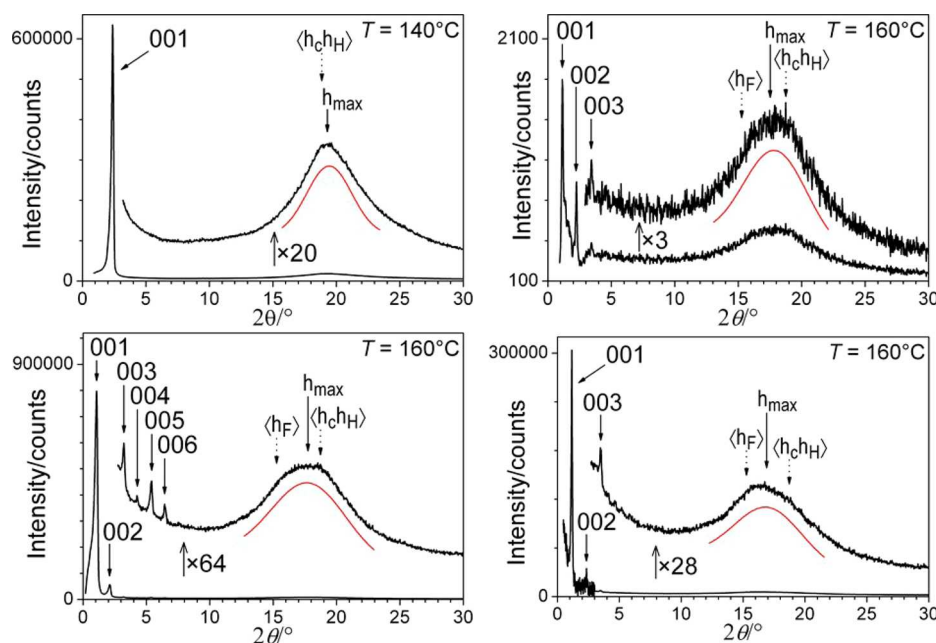


**Figure 3.** SAXS patterns of HH/H (SmC; top left), HH/F (SmC; top right), HH/F-b (SmC; bottom left), and HH/FF (SmC; bottom right); the small-angle part of HH/FF ( $<3^\circ$ ) comes from the image plate scan, and the wide-angle part is from acquisition with a gas-filled detector.

reduced intensity, once more due to the low contrast between fluorinated domains and ribbons of aggregated aromatic cores. In addition, the localized separation between fluorinated and hydrogenated domains leads to a loosely correlated, short-range periodicity  $D$  at  $\sim 19 \text{ \AA}$  ( $\xi = 25 \text{ \AA}$ ). Finally, the SAXS pattern of HH/HF is almost identical to that of HF/HF, which, again

combined with microscopy (Figure 2), confirms the Col<sub>h</sub> structure of the mesophase, and the loosely correlated domain structure is again seen in a midangle reflection ( $D = 19 \text{ \AA}$ ;  $\xi = 25 \text{ \AA}$ ).



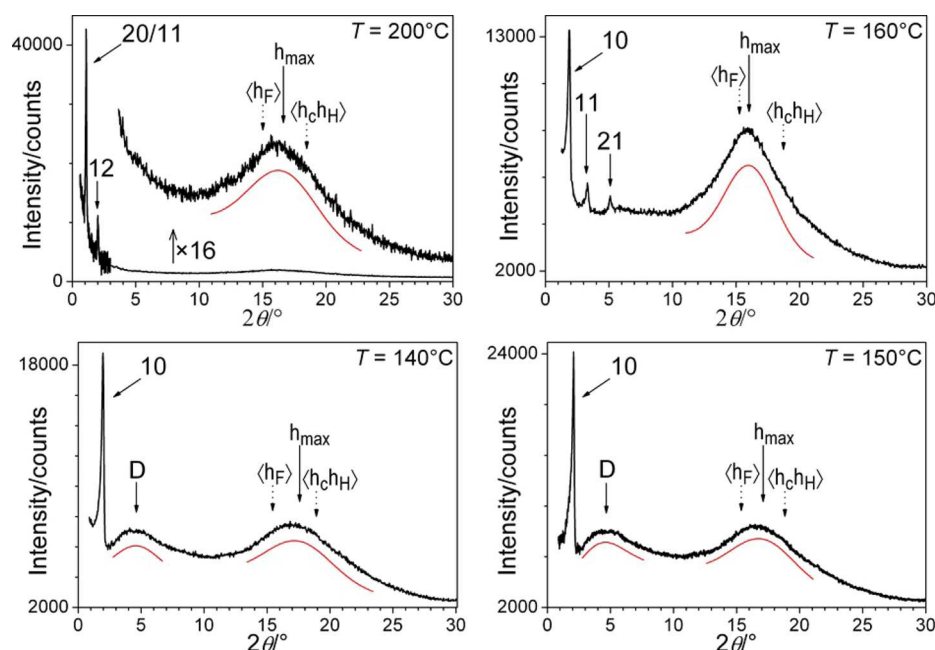


**Figure 4.** SAXS patterns of **HH/FF** ( $\text{Col}_h$ ; top left), **FF/FF** ( $\text{Col}_h$ ; top right), **HF/HF** ( $\text{Col}_h$ ; bottom left), and **HH/HF** ( $\text{Col}_h$ ; bottom right); the small-angle part of **HH/FF** ( $<3^\circ$ ) and **HH/HF** ( $<2.6^\circ$ ) comes from the image plate scan, and the wide-angle part is from acquisition with a gas-filled detector.

## DISCUSSION

Bearing hydrocarbon and fluorinated chains within the same molecular structure, it was anticipated that these mesogens may demonstrate the effects of hydrocarbon/fluorocarbon immiscibility within the mesomorphism of single compounds.<sup>53–55</sup> Smectic phases (i.e., lamellar phases with a planar interface) are found primarily for classical calamitic materials, with single alkyl chains at both ends of the rod-like mesogenic unit as the natural cross sections of chains ( $\sigma_H$ ) and the mesogen core ( $\sigma_C$ ) are very similar. However, where there is a significant mismatch between the cross sections of the core and the terminal chains as found in polycatenar compounds, then smectic phase formation can become disfavored, but this mismatch can be offset to some degree if there is significant tilting of the molecular core. This is indeed what occurs with tetracatenar mesogens and SmC phases when high tilt angles appear. However, such large tilts affect the lateral arrangement of the mesogen sublayers to accommodate the spatial requirements of the chains,<sup>56</sup> and above a certain point, the mesogen sublayers will eventually split into ribbons that define phases most commonly described as columnar.<sup>57</sup>

Thus, in tricatener mesogen **HH/H**, the presence of two terminal chains at one end causes tilting to form a SmC phase, and the difference in volume at the two ends may well be accounted for by some interdigitation or chain folding (the spacing is much shorter than the molecular length). Introducing a single, terminal fluorocarbon chain (**HH/F**) alleviates the difference in volume because the cross-sectional area of fluorocarbon chains is 50% greater than that of their hydrocarbon equivalents (Table 2).

The greater volume of the semiperfluorinated chain also modifies the lateral packing. Thus, the overall space requirement of the terminal chains of **HH/F** (single semiperfluorocarbon chain) can be regarded as intermediate between those of **HH/H** (single hydrocarbon chain) and **HH/HH** (two hydrocarbon chains) and therefore shows a SmC phase.

However, the nematic phase vanishes (common where there are fluorocarbon chains) and the smectic range extends a little with a slightly higher clearing point compared to that of the all-hydrocarbon compound **HH/H**, revealing improved confinement into layers in the presence of fluorinated tails.

SAXS data are consistent with assignment of the SmC phase as patterns show sharp, small-angle reflections from the lamellar periodicity as well as a broad, wide-angle scattering signal from liquid-like lateral distances inside of the layers. The lamellar periodicity trivially corresponds to a single mesogen/chain alternation in **HH/H** if a tilt angle of  $>60^\circ$  is assumed, but the periodicity doubles in the presence of the semiperfluorinated chain due to the requirement for formation of a bilayer structure owing to the mutual immiscibility of the two chain types (Figure 5). The numerous higher-order reflections visible for **HH/F** suggest well-defined layers with sharp interfaces between sublayers. Looking now to the other structural data for **HH/F**, the ratio of the statistical area effectively covered by chains and of their overall minimum cross section, that is, the chain packing ratio,  $q_H$ , stays quite close to unity ( $q_H \approx 1.15$ , Table 2), whereas the larger value for **HH/H** ( $q_H \approx 1.46$ ), combined with the absence of higher-order reflections, indicates a SmC phase with less well-defined layers analogous to the situation found in the SmC phase of more conventional calamitic mesogens, although with the possibility of layer undulations. As detailed previously for related polycatenar systems,<sup>44</sup> such undulations represent a low-energy compensation that offsets the cross-sectional mismatch, allowing the chain volume to be spread out laterally. The change in the molecular organization between **HH/H** and **HH/F** suggests that this mechanism is suppressed most likely due to segregation of the single semiperfluorocarbon chain ( $q_F \approx 1.55$ ), which limits the lateral expansion of the chain volume. Consistently, doubling of the semiperfluorocarbon chains in **HH/FF** imposes larger  $q_H$  values ( $\sim 1.46$ ) and reactivates the

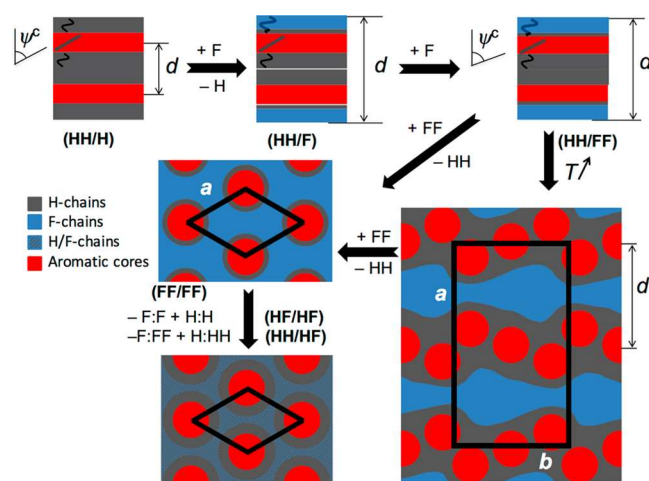


**Figure 5.** Schematic representation of the evolution of the molecular packing and the supramolecular organization in the mesophases as a function of the number, nature, and position of hydrocarbon and semiperfluorocarbon chains within the molecular structures of the series of polycatenar compounds **HH/H** to **HH/HF**; SmC phases (**HH/H**, **HH/F/HH/F-b**, **HH/FF**): mesogens are represented by gray rods, alkyl chains by black strips, and fluoroalkyl chains by blue strips; in the  $\text{Col}_h$  phase (**HH/FF**), the black frame is the rectangular lattice and  $d$  is the spacing of column rows; the red circles inside of gray domains schematize the cross sections of the columns formed by breakup of the layers of mesogens and surrounded by aliphatic spacers and tails (H), while the blue strips are regions of fluorinated chains (F). Note that the ribbons of mesogens are relatively free to adopt any orientation; therefore, they are averaged to circular columns in the mean lattice, and nothing is implied concerning organization of the mesogens within these columns. In the  $\text{Col}_h$  phases (**FF/FF**, **HF/HF**, **HH/HF**), the black diamond illustrates the hexagonal lattice; columns and aliphatic periphery are schematized by red circles and gray rings, respectively, and the peripheral continuum of F chains (**FF/FF**) or of mixed H/F chains (**HF/HF**, **HH/HF**) is colored in blue or hatched in gray/blue, respectively. Parameters are defined in Table 2.

lateral spreading and undulation mechanism, with the result that higher-order reflections almost vanish again.

Turning now to the tetracatenar materials, it is instructive to consider the effect of adding semiperfluorocarbon chains. Thus, addition of one such chain in the 3-position (**HH/HF**) leads to the observation of a  $\text{Col}_h$  phase, which is readily understood simply in terms of the increase in terminal chain volume. With this observation in hand, it would be expected that the addition of a second chain to give a 3,3'-disemiperfluorocarbon analogue (**HF/HF**) also leads to observation of a  $\text{Col}_h$  phase. Likewise then, compound **FF/FF** with four semiperfluorocarbon chains also shows a  $\text{Col}_h$  phase. In the case of **FF/FF**, it is possible to say something about the organization, which consists of ribbons of mesogens surrounded by a thin shell of an aliphatic spacer (tetramethylene spacer) and then a fluorinated peripheral continuum; the similarity in scattering length density between the mesogen core and the perfluorinated continuum explains the weakness of the first-order reflection. However, the presence of quite intense (11) and (21) reflections is also of note because tetracatenar systems with only hydrocarbon chains often give rise to patterns without higher-order reflections.<sup>44</sup> This feature implies well-defined and quite sharp interfaces consistent with the chain packing ratio,  $q_F$ , that is close to unity, revealing the close-packed nature of the fluorocarbon chains. The similarity in the hexagonal lattice parameter among **FF/FF**, **HF/HF**, and **HH/HF** (53.1, 51.1,

and 48.9 Å, respectively) shows that in the last two, the incompatibility of the hydrocarbon and fluorocarbon chains is accommodated readily to allow formation of the hexagonal phase. That said, the presence of the broad, midangle reflection,  $D$ , with a periodicity of 19 Å shows evidence for localized, periodic 'islands' of fluorocarbon that separate from the hydrocarbon chains, reflecting their mutual incompatibility. These islands moreover likely interfere with the cohesion between neighboring columns,<sup>58</sup> with larger islands causing greater interference, as evidenced by the lower transition temperatures observed for **HF/HF** with respect to **HH/HF**. This may account for differences in mesophase stability.

As discussed elsewhere,<sup>41,44</sup> layer undulations can be seen as a prelude to breaking up of the layered structure into ribbon-like phases, which are normally labeled as columnar of one sort or another, and this is seen in the thermal behavior of **HH/FF**, where the SmC phase gives way to a higher-temperature phase at 170 °C with a pseudofocal conic optical texture (Figure S3). By comparison with the wide literature on the subject, in polycatenar mesogens, this higher-temperature phase would be expected to be  $\text{Col}_h$ , but **HH/FF** bears two hydrocarbon chains at one end and two semiperfluorocarbon chains at the other, so that any organization beyond the SmC phase would need to accommodate its amphiphilic nature. In the SmC phase, the SAXS data again show the sharp interfaces (four orders of lamellar reflection), prevalent with terminal fluorocarbon chains, while in the higher-temperature phase, the loss of lamellar order is evidenced by a shift toward small angles of first-order periodicity and the appearance of a unique, higher-order reflection, and some other smaller-angle reflections with the wide-angle reflection remained unchanged. These reflections were tentatively indexed in a primitive rectangular lattice with  $a/b = \sqrt{3}$  and with large lattice parameters ( $a = 160.3$  Å,  $b = 92.5$  Å).<sup>41,44,59</sup> The formation of this rectangular lattice, which will for now be termed  $\text{Col}_r$ , then reflects the fact that the terminal chain volumes are too large to continue to accommodate a lamellar (SmC) phase, yet the amphiphilicity of the molecule means that it is unable to organize into a phase with hexagonal symmetry. Thus, the phase symmetry is reduced, and in order to accommodate the incompatibility of the two chain types, a large, rectangular lattice results. The lattice will then consist of the periodic alternation of strata of hydrocarbon and fluorocarbon continuums, the cores (columns) being found contiguous with the hydrocarbon chain continuum, and the periodicity of these strata (recognizing the formation of a double-layer structure) coincides with the first-order reflection inferring that the organization has a lamellar element (Figure 5). As such, while we persist with the  $\text{Col}_r$  nomenclature for the purposes of this discussion and for comparison with the wider literature, it is perhaps inappropriate to refer to the phase as columnar, rather we prefer to fall back on analogy with ribbon-like phases such as the SmA and B1 phases, both of which also have rectangular symmetry.<sup>60</sup> Despite the label  $\text{Col}_r$ , proposed in good faith and whose use is perpetuated in the literature, there is no regular, repeating 'slab' containing two or more molecules. Indeed, the data show that the cores of these molecules are absolutely not perpendicular to the 'column' direction and that the notion of the number of molecules,  $Z$ , in a repeat is little more than a calculation of a notional repeat distance based on hydrocarbon separation and column dimensions. As such, any value of  $Z$  obtained refers to an equivalent molecular volume rather than to whole, discrete molecules. Therefore the so-called columnar phases of

polycatenar molecules are more properly considered as ribbon phases. Making such a distinction does not in any way invalidate the earlier assumption concerning phases not being defined by the type of molecule of which they are composed for, as pointed out above, the  $\text{Col}_h$ ,  $\text{SmA}$ , and B1 phases are all in effect rectangular ribbon phases yet each arises from a different molecular type. The larger question is then how one might distinguish between the  $\text{Col}_h$  phase of disks and that of polycatenar materials. This matter requires greater reflection and a more wide-ranging discussion and will be reported elsewhere in due course.

A possible organizational model consistent with the structural information available for  $\text{HH/FF}$  is then proposed (Figure 5), and in considering it and the following description, it is important to stress that it is a static 2D projection of a dynamic 3D arrangement. Thus, the figure shows an effectively continuous ribbon in red representing the molecular cores surrounded by alkyl chains (gray). The alkyl area arises from the tetramethylene spacer at one end of the molecule and the alkyl chain at the other, and this is reflected in the differing thicknesses represented in the figure. The blue continuum is then the fluorocarbon fragment, and the larger apparent volume reflects the greater volume of fluorocarbon over hydrocarbon chain, as discussed earlier. The figure shows that the various interfaces are not planar (rather they undulate), which supports both the fact that the phase is formed above the SmC phase (volume mismatches and fluctuations drive the phase out of a simple lamellar arrangement consistent with all of the earlier published work on tetracatenar mesogens referenced throughout the paper) and also that  $q_F < 0$ . As argued previously, it can be the case that volume mismatches are accommodated by chains escaping out of the notional ribbon plane (not easily represented in a 2D figure), and of course, it is important to recall that the perfluoroalkyl segments of the chains are attached via a very flexible tetramethylene linker. Thus, the static, 2D projection in the figure shows differing apparent thicknesses of the different chain types, and where these are thinner, it can then be assumed that they escape into the third dimension.

## CONCLUSIONS

The present study has considered two families of polycatenar materials, in which one or more hydrocarbon chains have been replaced by semiperfluorocarbon chains. The resulting behavior is dominated by two effects. First, the fluorocarbon element of the chains occupies a greater volume than the hydrocarbon equivalent, and this is seen most clearly for the tetracatenar compounds where this increase in volume upon replacing hydrocarbon by fluorocarbon has a sufficient effect on the interfacial curvature to change from a lamellar (SmC) phase (13) into a  $\text{Col}_h$  phase ( $\text{FF/FF}$ ,  $\text{HF/HF}$ , and  $\text{HH/HF}$ ). The lattice parameters for these columnar phases are all very similar, showing that there are no other packing effects observed. Second, there is the mutual incompatibility between hydrocarbon and fluorocarbon chains and how this is accommodated when the molecules contain both. For the tricatener materials, the phase behavior with or without a fluorocarbon chain is a SmC phase, and the major difference observed is a doubling of the lamellar periodicity when a fluorocarbon chain is included as the system forms a bilayer, which keeps like chains with like. In the tetracatenar systems, it is more subtle. Replacing one hydrocarbon chain in a 3-position with its semiperfluorocarbon analogue ( $\text{HH/HF}$ ) tips the balance into  $\text{Col}_h$  from the SmC

phase, and this is also true when a second semiperfluorocarbon chain is added into the 3'-position ( $\text{HF/HF}$ ). As noted above, there is nothing remarkable about the lattice parameters in these  $\text{Col}_h$  phases, and therefore, these semiperfluorocarbon chains are evidently readily accommodated alongside their hydrocarbon equivalents. However,  $\text{HF/HF}$  and  $\text{HH/HF}$  do show a broad reflection (= loose correlation) corresponding to a 19 Å periodicity, which reveals the formation of regular islands of fluorocarbon in the structure reflecting the amphiphilic nature of these materials. Replacing the remaining two hydrocarbon chains ( $\text{FF/FF}$ ) also gives a compound with a  $\text{Col}_h$  phase but with no 19 Å periodicity as now there is only one type of terminal chain—semiperfluorocarbon. Compound  $\text{HH/FF}$  is isomeric with  $\text{HF/HF}$ , the difference being that the two semiperfluorocarbon chains in  $\text{HH/FF}$  are at one end of the molecule. Under these circumstances, the molecule shows a pronounced amphiphilicity so that the increase in chain volume destabilizes the SmC phase as expected. However, the need for like ends of the molecules to associate evidently precludes the formation of a phase with hexagonal symmetry, and rather, a phase of lower (rectangular) symmetry forms with large lattice parameters. One of the parameters is consistent with a lamellar bilayer, which suggests that the phase is ribbon-like and is also consistent with separation between the two chain types. It is important to note that the structural arguments used here are based on (i) a previous and very solid understanding of the organization in the mesophases of polycatenar systems, (ii) the availability from numerous studies of volumetric data from studies using dilatometry, and (iii) the availability of good-quality X-ray data analyzed in light of (i) and (ii).

## ASSOCIATED CONTENT

### Supporting Information

The Supporting Information is available free of charge on the ACS Publications website at DOI: 10.1021/acs.jpcb.7b04490.

Details of the equipment and methods used; description and details of the syntheses employed, including analytical data; description of the LC properties of the intermediate compounds (most of which are new); and representative optical textures for all of the final products (PDF)

## AUTHOR INFORMATION

### Corresponding Authors

\*E-mail: [bertrand.donnio@ipcms.unistra.fr](mailto:bertrand.donnio@ipcms.unistra.fr). Tel: (+33) 388107156 (B.D.).

\*E-mail: [duncan.bruce@york.ac.uk](mailto:duncan.bruce@york.ac.uk). Tel: (+44) 1904 324085 (D.W.B.).

### ORCID

Duncan W. Bruce: 0000-0002-1365-2222

### Present Address

\*A.G.: Department of Chemistry, Imperial College London, London SW7 2AZ, U.K.

### Notes

The authors declare no competing financial interest.

## ACKNOWLEDGMENTS

A.G. would like to acknowledge the Dinu Patriciu Foundation for sponsorship through the award of an 'Open Horizons' Excellence Studentship; M.C.T. thanks the National Sun Yat-sen University for provision of a scholarship, and B.D. and B.H.



thank the CNRS and the Université de Strasbourg for support. The authors thank Rachel Bean for acquiring some images in Figure 2.

## REFERENCES

- (1) Guittard, F.; Taffin de Givenchy, E.; Geribaldi, S.; Cambon, A. Highly Fluorinated Thermotropic Liquid Crystals: An Update. *J. Fluorine Chem.* **1999**, *100*, 85–96.
- (2) Kirsch, P. Fluorine in Liquid Crystal Design for Display Applications. *J. Fluorine Chem.* **2015**, *177*, 29–36.
- (3) Bremer, M.; Kirsch, P.; Klasen-Memmer, M.; Tarumi, K. The TV in Your Pocket: Development of Liquid-Crystal Materials for the New Millennium. *Angew. Chem., Int. Ed.* **2013**, *52*, 8880–8896.
- (4) Tschierske, C. Fluorinated Liquid Crystals: Design of Soft Nanostructures and Increased Complexity of Self-Assembly by Perfluorinated Segments. *Top. Curr. Chem.* **2011**, *318*, 1–108.
- (5) Pauling, L. *The Nature of the Chemical Bond and the Structure of Molecules and Crystals: An Introduction to Modern Structural Chemistry*; Cornell University Press: Ithaca, NY, 1940.
- (6) O'Hagan, D. Understanding Organofluorine Chemistry. An Introduction to the C-F Bond. *Chem. Soc. Rev.* **2008**, *37*, 308–31.
- (7) Arehart, S. V.; Pugh, C. Induction of Smectic Layering in Nematic Liquid Crystals Using Immiscible Components. 1. Laterally Attached Side-Chain Liquid Crystalline Poly(norbornene)s and Their Low Molar Mass Analogs with Hydrocarbon/Fluorocarbon Substituents. *J. Am. Chem. Soc.* **1997**, *119*, 3027–3037.
- (8) Shreenivasa Murthi, H. N.; Sadashiva, B. K. Influence of a Fluorine Substituent on the Mesomorphic Properties of Unsymmetrical Five-Ring Bent-Core Compounds. *J. Mater. Chem.* **2004**, *14*, 2813–2821.
- (9) Amaranatha Reddy, R.; Sadashiva, B. K. Influence of Fluorine Substituent on the Mesomorphic Properties of Five-Ring Ester Banana-Shaped Molecules. *Liq. Cryst.* **2003**, *30*, 1031–1050.
- (10) Eremin, A.; Wirth, I.; Diele, S.; Pelzl, G.; Schmalfuss, H.; Kresse, H.; Nadasi, H.; Fodor-Csorba, K.; Gacs-Baitz, E.; Weissflog, W. Structural Characterization of the New Polymorphic Mesophases Formed by Bent-Core Molecules. *Liq. Cryst.* **2002**, *29*, 775–782.
- (11) Hird, M. Fluorinated Liquid Crystals – Properties and Applications. *Chem. Soc. Rev.* **2007**, *36*, 2070–2095.
- (12) Shen, D.; Pegenau, A.; Diele, S.; Wirth, I.; Tschierske, C. Molecular Design of Nonchiral Bent-Core Liquid Crystals with Antiferroelectric Properties. *J. Am. Chem. Soc.* **2000**, *122*, 1593–1601.
- (13) Krafft, M. P.; Riess, J. G. Chemistry, Physical Chemistry, and Uses of Molecular Fluorocarbon-Hydrocarbon Diblocks, Triblocks, and Related Compounds - Unique “Apolar” Components for Self-Assembled Colloid and Interface Engineering. *Chem. Rev.* **2009**, *109*, 1714–1792.
- (14) Fleetwood, M. C.; McCoy, A. M.; Mecozzi, S. Synthesis and Characterization of Environmentally Benign, Semifluorinated Polymers and their Applications in Drug Delivery. *J. Fluorine Chem.* **2016**, *190*, 75–80.
- (15) Martin, O. M.; Yu, L.; Mecozzi, S. Solution Self-Assembly and Solid State Properties of Fluorinated Amphiphilic Calix[4]arenes. *Chem. Commun.* **2005**, *39*, 4964–4966.
- (16) Gladysz, J. A.; Curran, D. P.; Horváth, I. T. *Handbook of Fluorous Chemistry*; WILEY-VCH Verlag GmbH: Weinheim, Germany, 2004.
- (17) Riess, J. G. Fluorous Micro- and Nanophases with a Biomedical Perspective. *Tetrahedron* **2002**, *58*, 4113–4131.
- (18) Sadtler, V. M.; Giulieri, F.; Krafft, M. P.; Riess, J. G. Micellisation and Adsorption of Fluorinated Amphiphiles: Questioning the 1CF<sub>2</sub> ≈ 1.5CH<sub>2</sub> Rule. *Chem. - Eur. J.* **1998**, *4*, 1952–1956.
- (19) Percec, V.; Johansson, G.; Ungar, G.; Zhou, J. Fluorophobic Effect Induces the Self-Assembly of Semifluorinated Tapered Monodendrons Containing Crown Ethers into Supramolecular Columnar Dendrimers Which Exhibit a Homeotropic Hexagonal Columnar Liquid Crystalline Phase. *J. Am. Chem. Soc.* **1996**, *118*, 9855–9866.
- (20) Marczuk, P.; Lang, P.; Möller, M. Bulk Structure and Surface Activity of Semifluorinated Alkanes. *Colloids Surf., A* **2000**, *163*, 103–113.
- (21) Bondi, A. van der Waals Volumes and Radii. *J. Phys. Chem.* **1964**, *68*, 441–451.
- (22) Somasundaran, P. *Encyclopedia of Surface and Colloid Science*, 2nd ed.; Taylor and Francis Group: Boca Raton, FL, 2006, Vol. 4.
- (23) Law, C.-K. E.; Horváth, I. T. Synthesis and Applications of Fluorous Phosphines. *Org. Chem. Front.* **2016**, *3*, 1048–1062.
- (24) Atwood, D. A. *Sustainable Inorganic Chemistry*; Wiley: West Sussex, U.K., 2016.
- (25) Baker, R. T.; Tumas, W. Toward Greener Chemistry. *Science* **1999**, *284*, 1477–1479.
- (26) de Gracia Lux, C.; Donnio, B.; Heinrich, B.; Krafft, M. P. Thermal Behavior and High- and Low-Temperature Phase Structures of Gemini Fluorocarbon/Hydrocarbon Diblocks. *Langmuir* **2013**, *29*, 5325–5336.
- (27) Bury, I.; Heinrich, B.; Bourgoigne, C.; Mehl, G. H.; Guillon, D.; Donnio, B. Self-Assembly and Liquid-Crystalline Supramolecular Organisations of Semifluorinated Block Co-Dendritic Molecules. *New J. Chem.* **2012**, *36*, 452–468.
- (28) Date, R. W.; Iglesias, E. F.; Rowe, K. E.; Elliott, J. M.; Bruce, D. W. Metallomesogens by Ligand Design. *Dalton Trans.* **2003**, 1916, 1914–1931.
- (29) Höpken, J.; Möller, M. On the Morphology of (Perfluoroalkyl)-alkanes. *Macromolecules* **1992**, *25*, 2482–2489.
- (30) Viney, C.; Russell, T. P.; Depero, L. E.; Twieg, R. J. Transitions to Liquid Crystalline Phases in a Semifluorinated Alkane. *Mol. Cryst. Liq. Cryst.* **1989**, *168*, 63–82.
- (31) Viney, C.; Twieg, R. J.; Russell, T. P.; Depero, L. E. The Structural Basis of Transitions between Highly Ordered Smectic Phases in Semifluorinated Alkanes. *Liq. Cryst.* **1989**, *5*, 1783–1788.
- (32) Pelzl, G.; Diele, S.; Lose, D.; Ostrovski, B. I.; Weissflog, W. The Influence of the Shape and the Incompatibility of Molecular Moieties on the Structure of Smectic Mesophases. *Cryst. Res. Technol.* **1997**, *32*, 99–109.
- (33) Lose, D.; Diele, S.; Pelzl, G.; Dietzmann, E.; Weissflog, W. Frustrated Smectic Phases in Swallow-Tailed Compounds with Perfluorinated Chains. *Liq. Cryst.* **1998**, *24*, 707–717.
- (34) Pegenau, A.; Hong Cheng, X.; Tschierske, C.; Göring, P.; Diele, S. Formation of Mesophases Based on Micro-Segregation: Columnar Liquid-Crystalline Phases of First Generation Dendrimers with Perfluorinated Segments. *New J. Chem.* **1999**, *23*, 465–467.
- (35) Cheng, X. H.; Das, M. K.; Diele, S.; Tschierske, C. Influence of Semiperfluorinated Chains on the Liquid Crystalline Properties of Amphiphilic Polyols: Novel Materials with Thermotropic Lamellar, Columnar, Bicontinuous Cubic, and Micellar Cubic Mesophases. *Langmuir* **2002**, *18*, 6521–6529.
- (36) Cheng, X. H.; Diele, S.; Tschierske, C. Molecular Design of Liquid-Crystalline Block Molecules: Semifluorinated Pentaerythritol Tetrabenzoates Exhibiting Lamellar, Columnar and Cubic Mesophases. *Angew. Chem., Int. Ed.* **2000**, *39*, 592–595.
- (37) Kohlmeier, A.; Janietz, D. Hydrogen-Bonded Block Mesogens Derived from Semiperfluorinated Benzoic Acids and the Non-Mesogenic 1,2-bis(4-pyridyl)ethylene. *Liq. Cryst.* **2007**, *34*, 65–71.
- (38) Malthête, J.; Nguyen, H. T.; Destrade, C. Phasmids and Polycatenar Mesogens. *Liq. Cryst.* **1993**, *13*, 171–187.
- (39) Nguyen, H. T.; Destrade, C.; Malthête, J. Phasmids and Polycatenar Mesogens. *Adv. Mater.* **1997**, *9*, 375–388.
- (40) Fazio, D.; Mongin, C.; Donnio, B.; Galerne, Y.; Guillon, D.; Bruce, D. W. Bending and Shaping: Cubics, Calamitics and Columnars. *J. Mater. Chem.* **2001**, *11*, 2852–2863.
- (41) Guillon, D.; Heinrich, B.; Ribeiro, A. C.; Cruz, C.; Nguyen, H. T. Thermotropic Lamellar-to-Columnar Phase Transition Exhibited by a Biforked Compound. *Mol. Cryst. Liq. Cryst. Sci. Technol., Sect. A* **1998**, *317*, 51–64.
- (42) Donnio, B.; Bruce, D. W. Liquid-Crystalline Complexes of Palladium(II) and Platinum(II) with Di- and Tri-alkoxystilbazoles:

Ligand Control of Mesomorphism. *J. Chem. Soc., Dalton Trans.* **1997**, 2745–2755.

(43) Donnio, B.; Heinrich, B.; Allouchi, H.; Kain, J.; Diele, S.; Guillon, D.; Bruce, D. W. A Generalized Model for the Molecular Arrangement in the Columnar Mesophases of Polycatenar Mesogens. Crystal and Molecular Structure of Two Hexacatenar Mesogens. *J. Am. Chem. Soc.* **2004**, *126*, 15258–15268.

(44) Smirnova, A. I.; Heinrich, B.; Donnio, B.; Bruce, D. W. The Influence of Lateral Fluorination and Cyanation on the Mesomorphism of Polycatenar Mesogens and the Nature of the SmC Phase Therein. *RSC Adv.* **2015**, *5*, 75149–75159.

(45) Alvey, L. J.; Meier, R.; Soos, T.; Bernatis, P.; Gladysz, J. A. Syntheses and Carbonyliridium Complexes of Unsymmetrically Substituted Fluorous Trialkylphosphanes: Precision Tuning of Electronic Properties, Including Insulation of the Perfluoroalkyl Groups. *Eur. J. Inorg. Chem.* **2000**, *2000*, 1975–1983.

(46) Johansson, G.; Percec, V.; Ungar, G.; Zhou, J. Fluorophobic Effect in the Self-Assembly of Polymers and Model Compounds Containing Tapered Groups into Supramolecular Columns. *Macromolecules* **1996**, *29*, 646–660.

(47) Luscombe, C. K.; Proemmel, S.; Huck, W. T. S.; Holmes, A. B.; Fukushima, H. Synthesis of Supercritical Carbon Dioxide Soluble Perfluorinated Dendrons for Surface Modification. *J. Org. Chem.* **2007**, *72*, 5505–5513.

(48) Percec, V.; Glodde, M.; Peterca, M.; Rapp, A.; Schnell, I.; Spiess, H. W.; Bera, T. K.; Miura, Y.; Balagurusamy, V. S. K.; Aqad, E.; Heiney, P. A. Self-Assembly of Semifluorinated Dendrons Attached to Electron-Donor Groups Mediates Their  $\pi$ -Stacking via a Helical Pyramidal Column. *Chem. - Eur. J.* **2006**, *12*, 6298–6314.

(49) Smirnova, A. I.; Zharnikova, N. V.; Donnio, B.; Brus, D. W. The Influence of Lateral Apolar Substituents on the Mesomorphic Behaviour of Tetracatenar Liquid Crystals. *Russ. J. Gen. Chem.* **2010**, *80*, 1331–1340.

(50) Marcos, M.; Giménez, R.; Serrano, J. L.; Donnio, B.; Heinrich, B.; Guillon, D. Dendromesogens: Liquid Crystal Organisations of Poly(amidoamine) Dendrimers versus Starburst Structures. *Chem. - Eur. J.* **2001**, *7*, 1006–1013.

(51) Myśliwiec, D.; Donnio, B.; Chmielewski, P. J.; Heinrich, B.; Stepień, M. Peripherally Fused Porphyrins via the Scholl Reaction: Synthesis, Self-Assembly, and Mesomorphism. *J. Am. Chem. Soc.* **2012**, *134*, 4822–4833.

(52) Alameddine, B.; Aebischer, O. F.; Heinrich, B.; Guillon, D.; Donnio, B.; Jenny, T. A. Influence of Linear and Branched Perfluoroalkylated Side Chains on the  $\pi$ - $\pi$  Stacking Behaviour of Hexa-peri-hexabenzocoronene and Thermotropic Properties. *Supramol. Chem.* **2014**, *26*, 125–137.

(53) Tschierske, C. Liquid Crystal Engineering – New Complex Mesophase Structures and their Relations to Polymer Morphologies, Nanoscale Patterning and Crystal Engineering. *Chem. Soc. Rev.* **2007**, *36*, 1930–1970.

(54) Nishikawa, E.; Yamamoto, J.; Yokoyama, H. Nano-Segregated Structures of Hydrogen-Bonded Mesogens with Perfluorinated Moieties: Cubic Phase Formation and First Order Smectic A to Smectic C Phase Transition. *Liq. Cryst.* **2003**, *30*, 785–798.

(55) Nishikawa, E.; Yamamoto, J.; Yokoyama, H. Polycatenar Mesogens with a Perfluorinated Moiety Showing Liquid Crystalline Polymorphism and, Microscopically, a Continuous Smectic A to Structured, Fluid, Optically Isotropic Phase Transition. *J. Mater. Chem.* **2003**, *13*, 1887–1893.

(56) Allouchi, H.; Cotrait, M.; Guillon, D.; Heinrich, B.; Nguyen, H. T. Relationships between the Crystalline and the Smectic C Structures of a Biforked Mesogen. *Chem. Mater.* **1995**, *7*, 2252–2258.

(57) Nguyen, H. T.; Destrade, C.; Levelut, A. M.; Malthête, J. Biforked Mesogens: A New Type of Thermotropic Liquid Crystals. *J. Phys. (Paris)* **1986**, *47*, 553–557.

(58) Pitto-Barry, A.; Barry, N. P. E.; Russo, V.; Heinrich, B.; Donnio, B.; Therrien, B.; Deschenaux, R. Designing Supramolecular Liquid-Crystalline Hybrids from Pyrenyl-Containing Dendrimers and Arene Ruthenium Metallacycles. *J. Am. Chem. Soc.* **2014**, *136*, 17616–17625.

(59) Ribeiro, A. C.; Heinrich, B.; Cruz, C.; Nguyen, H. T.; Diele, S.; Schröder, M. W.; Guillon, D. Rectangular to Hexagonal Columnar Phase Transition Exhibited by a Biforked Mesogen. *Eur. Phys. J. E: Soft Matter Biol. Phys.* **2003**, *10*, 143–151.

(60) Nguyen, H. T.; Destrade, C.; Allouchi, H.; Bideau, J. P.; Cotrait, M.; Guillon, D.; Weber, P.; Malthête, J. Phasmod and Biforked Mesogens with Thiobenzoate End Groups. *Liq. Cryst.* **1993**, *15*, 435–449.